

Ab initio density functional study of phase stability and noncollinear magnetism in Mn

This article has been downloaded from IOPscience. Please scroll down to see the full text article.

2001 J. Phys.: Condens. Matter 13 L681

(<http://iopscience.iop.org/0953-8984/13/28/104>)

View [the table of contents for this issue](#), or go to the [journal homepage](#) for more

Download details:

IP Address: 171.66.16.226

The article was downloaded on 16/05/2010 at 13:56

Please note that [terms and conditions apply](#).

LETTER TO THE EDITOR

Ab initio* density functional study of phase stability and noncollinear magnetism in Mn*D Hobbs and J Hafner**

Institut für Materialphysik and Centre for Computational Materials Science, Universität Wien, Sensengasse 8/12, A-1090 Wien, Austria

Received 25 May 2001

Published 29 June 2001

Online at stacks.iop.org/JPhysCM/13/L681**Abstract**

The crystalline and magnetic structures of all known polymorphs of Mn have been investigated using generalized spin-density functional theory based on an unconstrained vector-field description of the magnetization density. We find that at atomic volumes smaller than 12 \AA^3 , the magnetic ground state of α -Mn is collinear with magnetic moments ranging between 0 and $3 \mu_B$ depending on the local symmetry of the atomic positions. At larger atomic volumes, a metastable collinear configuration coexists with a stable noncollinear state. The noncollinearity of the magnetic structure is driven by the appearance of magnetic moments on sites IV, leading to a frustration of exchange interactions in local triangular configurations. A similar situation is found in β -Mn, with a collinear structure with coexisting magnetic and nonmagnetic sites. The α -phase is found to be stable over a wide range of volumes; under compression a phase transition to hexagonal ϵ -Mn is predicted.

From the point of view of its structural and magnetic properties, Mn can be considered as the most complex of all metallic elements. As a group-VII element Mn would be expected, according to the regular structural trends in the series of the 4d and 5d transition metals, to crystallize in a hexagonal close-packed (hcp) structure [1]. It is well known, however, that the magnetism of the 3d elements disturbs this regular structural sequence. While for Fe and Co, magnetism merely stabilizes the body-centred cubic (bcc) and the hcp structure respectively instead of the hcp and face-centred cubic (fcc) structures of the 4d and 5d homologues, Mn behaves in a totally different way. α -Mn, the most stable polymorph under normal conditions of temperature and pressure, has an exotic crystal structure containing 58 atoms in a cubic unit cell (space group $T_d^3 - I\bar{4}3m$) [2]. β -Mn exists in the temperature interval from 1000 K to 1368 K and is simple cubic with twenty atoms per unit cell (space group $P4_132$) [3, 4]. The fcc γ -phase is found in the high-temperature region between 1368 K and 1406 K; at higher temperatures up to the melting point of $T_M = 1517$ K the δ -phase has the bcc structure. Recent high-pressure studies [5] found a structural phase transition from α -Mn to an as yet not

completely characterized phase. On the basis of a new diffraction peak appearing above the transition pressure of 165 GPa, it has been suggested that the new phase might be bcc but on the basis of density functional calculations it was argued that the high-pressure phase ϵ -Mn is hcp, in agreement with the stable crystal structures of Tc and Re [6].

Magnetic ordering adds to the bewildering structural complexity of Mn. α -Mn undergoes a paramagnetic-to-antiferromagnetic phase transition at the Néel temperature of $T_N = 95$ K. The magnetic transition is coupled to a tetragonal distortion; neutron diffraction data indicate that the magnetic structure is anti-body-centred (space group $I\bar{4}2m$) leading to an increase of the crystallographically inequivalent atomic positions from four to six [7]. The different atomic sites are also magnetically inequivalent: neutron scattering [7, 8], magnetic torque measurements [9] and nuclear magnetic resonance (NMR) investigations [10] agree on a non-collinear antiferromagnetic structure with large magnetic moments on sites I and II and much smaller moments on the remaining positions—sites IVa and IVb could be occupied even by nonmagnetic Mn atoms. One explanation for the stability of the α -Mn structure postulates indeed that the Mn atoms with different magnetic and electronic configurations behave like atoms with different sizes [11]—a point of view which is suggested by the analogy of the α -Mn and the χ -phase structures (adopted, e.g., by intermetallic compounds such as $\text{Al}_{12}\text{Mg}_{17}$ or $\text{Fe}_{36}\text{Cr}_{12}\text{Mo}_{10}$).

The properties of β -Mn are hardly less complex. In the simple cubic cell there are two inequivalent sites. The magnetic characterization of β -Mn has shown that only one type of site carries a small magnetic moment, the other sites being essentially nonmagnetic [12, 13]. The magnetic properties of γ - and δ -Mn can be studied only in samples produced by rapid quenching; both order antiferromagnetically.

While the structural and magnetic properties of the ferromagnetic metals Fe, Co and Ni are now thoroughly well explained on the basis of local spin-density (LSD) theory including generalized gradient corrections (GGCs) (see, e.g., Moroni *et al* [14] and references therein), the incommensurate spin-density-wave ground state of bcc Cr [15] and the complex magnetic configurations of α - and β -Mn continue to defy theoreticians. For the simpler γ -, δ - and ϵ -phases, *ab initio* LSD calculations of phase stabilities and magnetic properties yield good agreement with experiment on samples produced by quenching or epitaxial growth if GGCs are included in the exchange–correlation functional [6, 16, 17]. An important result is the evidence for a competition between high- and low-spin states in these phases. For α - and β -Mn, however, LSD investigations have been restricted to calculations of the collinear antiferromagnetic structures at the experimental density and crystal structure [18, 19]. A high-spin state of the Mn atoms at sites I and II and a marginally magnetic character of those on sites III and IV are predicted in agreement with experiment, but nothing could be said about phase stability and the correlation between the magnetic and geometric structures.

Due to the recent progress in DFT, noncollinear magnetic structures can now be treated at various levels of sophistication:

- (i) within an atomic-sphere approximation, the spin density has spherical symmetry within the overlapping atomic spheres, within each sphere the direction of the magnetic moment is fixed [20, 21];
- (ii) within a full-potential linearized augmented-plane-wave (FLAPW) approach, the quantization axis is fixed only within the almost touching muffin-tin spheres; magnetization density and exchange field are described as vector fields in the interstitial region [22]; and
- (iii) a projector-augmented-wave (PAW) approach [23, 24] allows for a fully unconstrained vector-field description of noncollinear magnetism [25].

In the present work we report the results of *ab initio* DFT calculations of the crystal structure, phase stability and magnetic ordering of all known polymorphs of Mn using the PAW method as implemented in the Vienna *ab initio* simulation package VASP [24, 25]. Exchange and correlation are described in the LSD + GGA approximation, using the LSD functional of Perdew and Zunger [26], supplemented with the gradient corrections proposed by Perdew *et al* [27]. The optimization of the atomic geometry (ionic coordinates, shape and volume of the unit cell) is performed via a conjugate-gradient minimization of the total energy, using the Hellmann–Feynman forces on the atoms and the stresses on the unit cell. The magnetization density (magnitude and direction) is calculated self-consistently on a fine FFT grid for the plane-wave part and on radial support grids for the contributions from the augmentation and compensation charges. For visualization of the results only, local magnetic moments are calculated by projecting the plane-wave components of the orbitals onto spherical waves inside atomic spheres and averaging magnitude and direction inside each sphere. Initial magnetic configurations were chosen in a collinear low-moment configuration and also close to the noncollinear magnetic structure, both being derived from experiments.

Figures 1 and 2 summarize our results for α -Mn: figure 1 shows the total energies of paramagnetic and both collinear and noncollinear antiferromagnetic α -Mn as functions of volume, figure 2 the variation of the axial ratio and of the internal coordinates. For atomic volumes up to about 12 \AA^3 the structure remains cubic and independent of the starting configuration, while the magnetic structure relaxes to a collinear magnetic configuration with zero magnetic moment on sites IV. For larger volumes, a metastable collinear magnetic configuration coexists with the stable noncollinear configuration. In the collinear configuration we observe a tetragonal distortion of up to two per cent (i.e. much larger than observed experimentally), accompanied by a pronounced splitting of the internal coordinates of sites III and IV into two groups. The magnetic moments on sites IVa and IVb develop only very slowly on expansion. The stable noncollinear magnetic configuration could be found only by relaxation at an expanded volume ($\geq 15 \text{ \AA}^3$) and using a rescaled magnetic configuration as the starting point for the optimization at increased density. In this noncollinear configuration, the tetragonal distortion is much more modest (in good agreement with the neutron diffraction data of Lawson *et al* [7]; see figure 2), but large moments develop at sites IV and the frustrated exchange interaction causes the moments on sites III and IV to cant away from their preferred direction in the collinear structure. The full noncollinear spin structure is shown in figure 3.

The mechanism driving the formation of a noncollinear spin structure is clearly related to the crystalline structure of α -Mn: the atoms at sites I and II carrying large collinear moments (see figure 3(a)) have coordination number (CN) 16. The CN16 Friauf polyhedron around sites I at the corners and in the centre of the unit cell consists of a tetrahedron of type-II atoms and a truncated tetrahedron whose twelve vertices are occupied by type-IV atoms. The relative orientation of the tetrahedron and the truncated tetrahedron is such that the type-II atoms are placed just out from the centre of the hexagonal faces. The distances between the type-IV atoms located on the small triangular faces of the truncated tetrahedron (see figure 3(b)) are the smallest interatomic distances in the α -Mn lattice. The strong frustration of the antiferromagnetic exchange interactions in the triangular configuration leads to a complete quenching of the magnetic moments on sites IV at high density; at larger volumes the relative orientation of the moments in these triangles is as expected for a frustrated triangular structure, i.e. we find approximately 120° angles between nearest-neighbour moments. The appearance of nonzero moments on sites IV also leads to a strong frustration of the interaction with the moments on sites III. This is shown in figure 3(c) where we see that in parallel with the increasing size of the type-IV moments the type-III moments rotate away from their orientation collinear to the moments on sites I and II. In the metastable collinear structure, the frustration

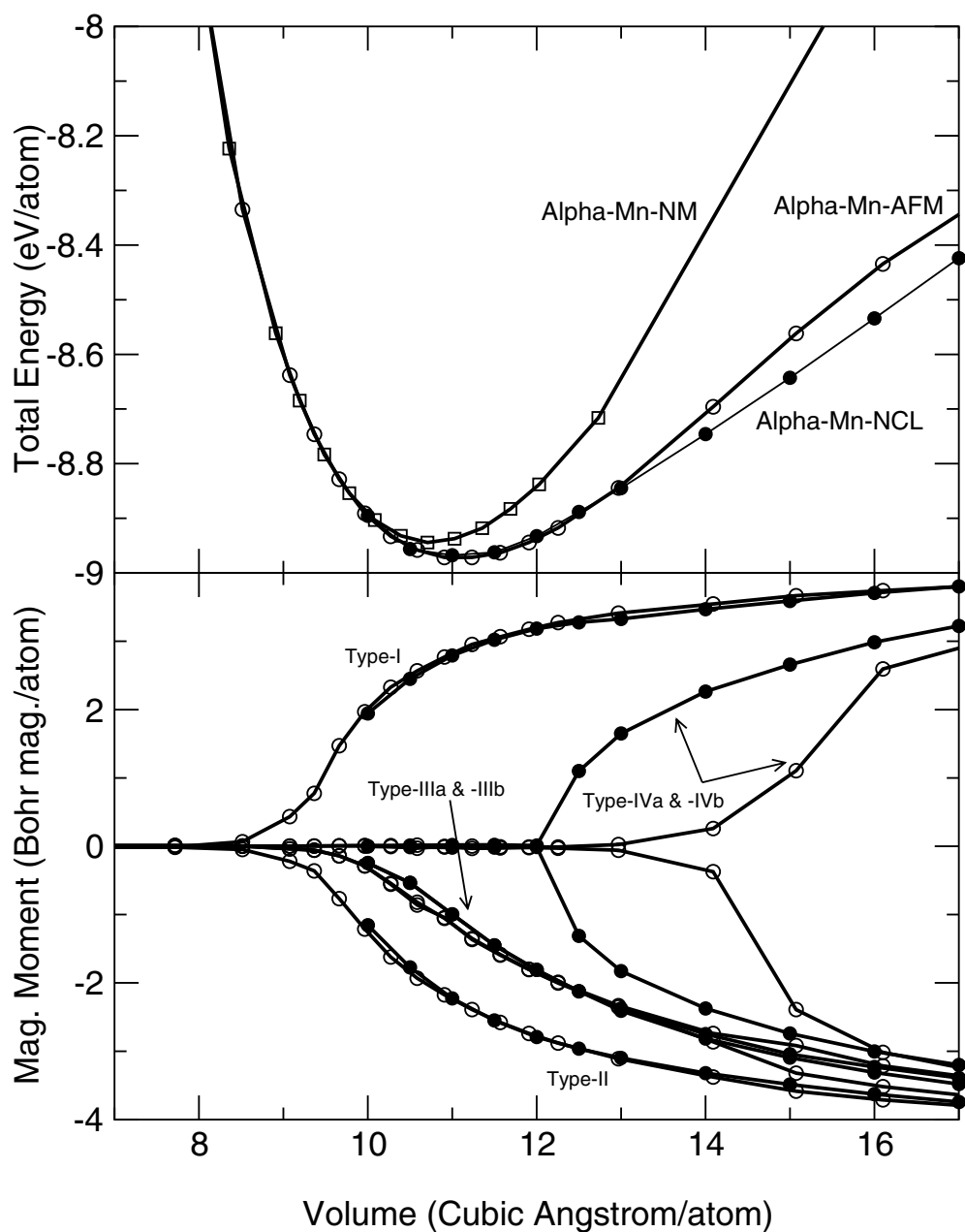


Figure 1. (a) Total energies of nonmagnetic and both collinear and noncollinear antiferromagnetic α -Mn as functions of volume. At atomic volumes larger than about 12 \AA^3 , a metastable collinear antiferromagnetic configuration coexists with a stable noncollinear magnetic structure (open and closed circles, respectively). (b) Variations of the local magnetic moments m_i as functions of volume. For the noncollinear case the absolute values $|\bar{m}_i|$ of the local moments, multiplied by the sign of its projection on \bar{m}_i , are displayed.

in the triangular units of type-IV atoms is relaxed by a strong structural distortion leading to short and long distances within each triangle.

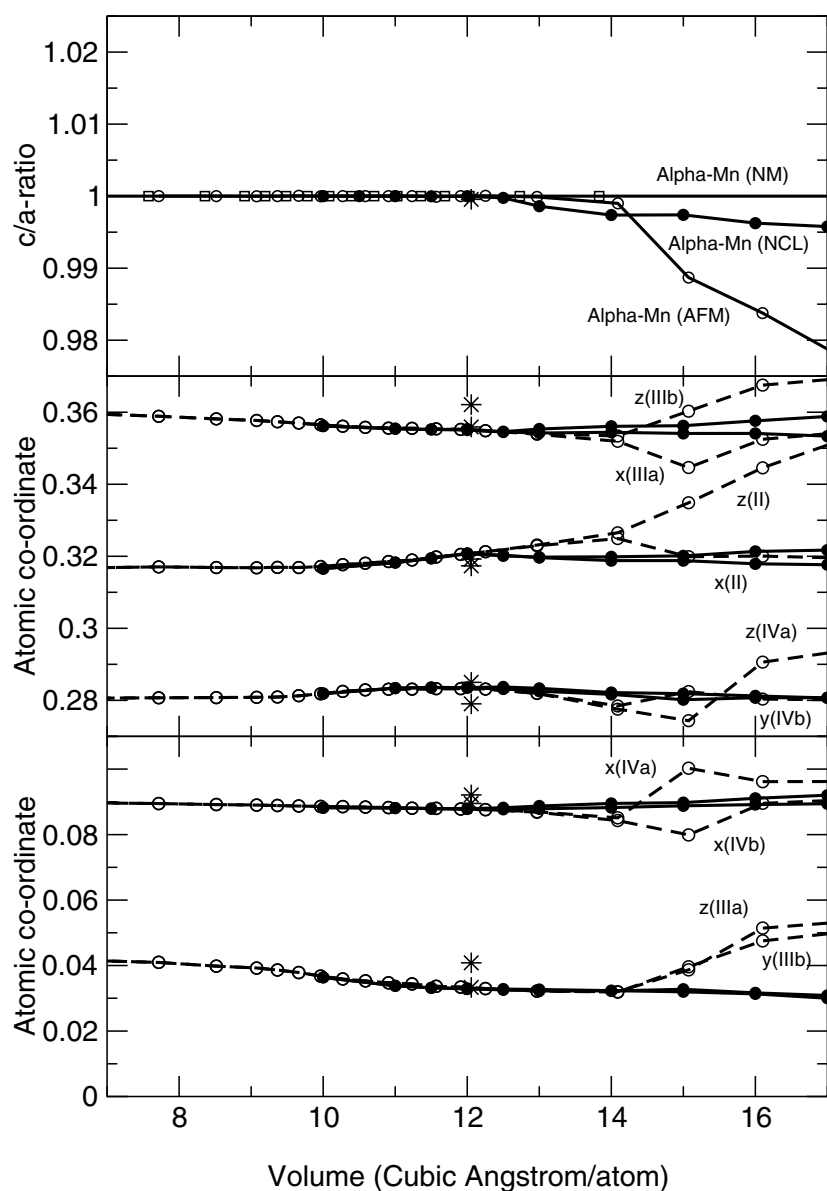


Figure 2. Variations of the axial ratio c/a (a) and of the internal coordinates of sites II, III and IV (b) with volume. Open and closed circles represent the results for the collinear and noncollinear magnetic configurations, respectively. Experimental values are represented by asterisks, after reference [7].

The calculated noncollinear structure compares well with the structure proposed on the basis of the magnetic neutron diffraction, although the analysis is quite sensitive to assumptions on the magnetic form factor (Lawson *et al* [7] assume that the form factor is the same on all sites—which is hardly compatible with the present analysis). At the experimental atomic volume of 12.05 \AA^3 , the calculated absolute values of the moments at sites I to IV are 3.19 (3.276), 2.79 (2.964), 1.81 (2.12) and 0.0 (1.31/1.10) μ_B , respectively. Numbers in parentheses

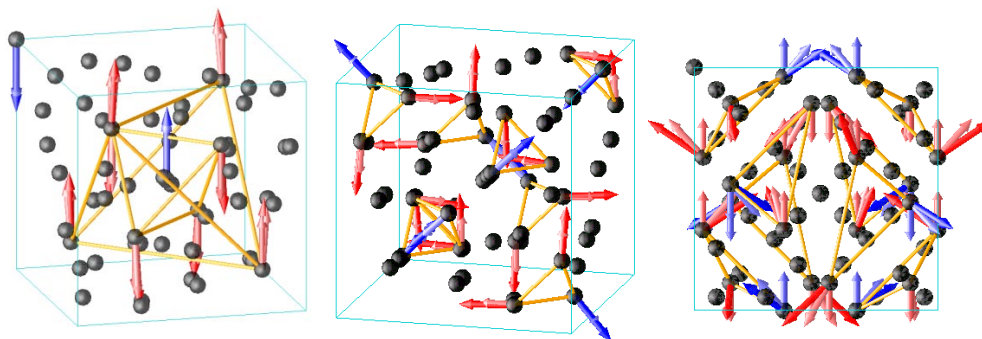


Figure 3. Noncollinear magnetic structure of α -Mn. Left panel: magnetic moments on sites I (blue arrows) and sites II (purple arrows), viewed slightly away from the top. Arrows of different length and shading indicate the increase of the moments on expansion. Middle panel: magnetic moments on the type-IV atoms (blue—IVa, purple—IVb), viewed slightly away from the front. The yellow bars mark the short interatomic distances between atoms forming the small triangular faces of the truncated tetrahedron. Right panel: moments on sites III (blue—IIIa, purple—IIIb), top view. Note how with increasing volume the moments rotate away from the direction collinear to the moments on sites I and II. See the text.

refer to a slightly expanded volume of 12.5 \AA^3 . The corresponding values given by Lawson *et al* [7] are 2.83, 1.82, 0.43/0.32 and $0.45/0.48 \mu_B$; Yamagata and Asayama [10] report moments of 2.05, 1.84/1.75, 0.62/0.57 and $0.22/0.31 \mu_B$. Hence within the uncertainty of the experimental values we note reasonable agreement between theory and experiment; the most important remaining difference is that the magnetism on sites IV and the correlated noncollinearity appear only at a volume that is slightly expanded compared to the experimental one. A detailed comparison must be left to a more extended publication.

We have also studied the structural and magnetic properties of the β -phase. Around the equilibrium density we find very small moments of about $0.2 \mu_B$ on sites I, while atoms of type II are essentially nonmagnetic, i.e. β -Mn is found to be marginally ferrimagnetic. A striking feature is the very slow disappearance of the magnetic moments at sites I on compression. This correlates rather well with reports of strong antiferromagnetic spin fluctuations in β -Mn [12]. Again the quenching of the magnetic moments can be ascribed to geometric frustrations of the antiferromagnetic exchange interactions—Nakamura *et al* have stressed the analogy of the interactions in the site-II sublattice with those on an antiferromagnetic Kagomé lattice. Details will be presented elsewhere.

Finally we analyse the relative stability of the various polymorphs of Mn. Figure 4 reports the total energies of α -, β -, γ -, δ - and ϵ -Mn as functions of volume. We find, in agreement with experiment, that α -Mn is the stable polymorph over a wide range of atomic volumes. The β -phase is found to have the second lowest energy, the structural energy difference being $\Delta E/(\beta - \alpha) = 0.06 \text{ eV/atom}$. Under sufficient compression we predict a sluggish phase transition to the hexagonal ϵ -phase at a pressure of 200–300 kbar. Details of the phase stability calculations will be reported elsewhere.

In summary, the exceptional properties of Mn can be related to the fact that the 3d band is just half-filled: on one hand this means that only bonding d states are occupied and hence the interatomic bond strength is maximized; on the other hand according to Hund's third rule the spin moment is also maximum and this favours expansion. In the simpler γ -, δ - and ϵ -phases these conflicting tendencies lead to the competition between high- and low-spin states, in the more complex α - and β -phases to the coexistence of large high-moment atoms and small

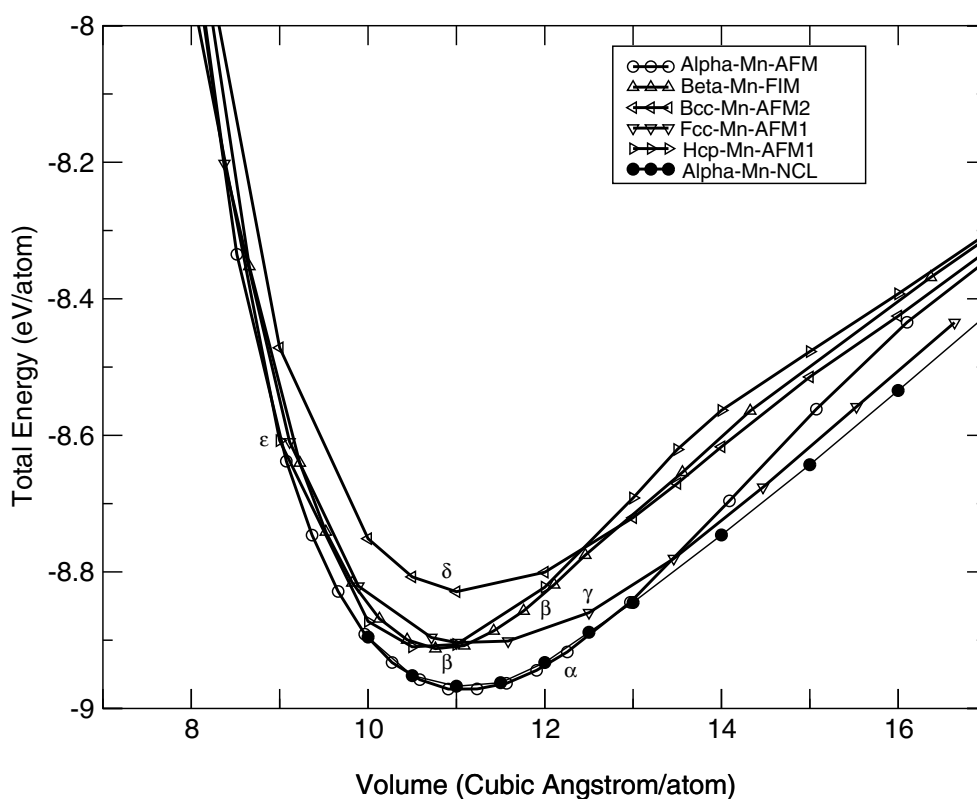


Figure 4. Total energies of the five polymorphs of Mn as functions of volume. For α -Mn the full circles represent the energy of the noncollinear phase, the empty circles that of the collinear phase (which is only metastable upon expansion).

nonmagnetic or low-moment atoms whose topologically close-packed arrangement allows maximization of the packing density. The noncollinear spin structure results from the fact that without a complete quenching of the moments on sites IV some local frustration in local triangular groups of atoms survives. Here we have shown that generalized LSD calculations involving an unconstrained vector-field description of magnetization density and exchange field allow for a quantitatively accurate prediction of the atomic and magnetic structures of the most complex of all metallic elements.

This was performed within the TMR-Network 'Electronic structure calculations for industry and basic sciences' (Contract FMRX-CT98-0178).

References

- [1] Donohue J 1974 *The Structures of the Elements* (New York: Wiley)
- [2] Bradley A J and Thewlis J 1927 *Proc. R. Soc. A* **115** 465
- [3] Preston G D 1928 *Phil. Mag.* **5** 1207
- [4] O'Keefe M and Anderson S 1977 *Acta Crystallogr. A* **33** 914
- [5] Fujihisa H and Takemura K 1995 *Phys. Rev. B* **52** R13 257
- [6] Zheng-Johansson J X *et al* 1998 *Phys. Rev. B* **57** 10989
- [7] Lawson A C *et al* 1994 *J. Appl. Phys.* **76** 7049

-
- [8] Yamada T *et al* 1970 *J. Phys. Soc. Japan* **28** 615
 - [9] Yamada T and Tazawa S 1970 *J. Phys. Soc. Japan* **28** 609
 - [10] Yamagata H and Asayama K 1972 *J. Phys. Soc. Japan* **33** 400
 - [11] Brewer L 1968 *Science* **161** 115
 - [12] Nakamura H *et al* 1997 *J. Phys.: Condens. Matter* **9** 4701
 - [13] Canals B and Lacroix C 2000 *Phys. Rev. B* **61** 11 251
 - [14] Moroni E G, Kresse G, Furthmüller J and Hafner J 1997 *Phys. Rev. B* **56** 15 629
 - [15] Zabel H 1999 *J. Phys.: Condens. Matter* **11** 9303
Hafner R *et al* 2001 *J. Phys.: Condens. Matter* **13** L239
 - [16] Asada T and Terakura K 1993 *Phys. Rev. B* **47** 15 992
 - [17] Eder M, Hafner J and Moroni E G 2000 *Phys. Rev. B* **61** 11 492
 - [18] Sliwko V, Mohn P and Schwarz K 1994 *J. Phys.: Condens. Matter* **6** 6557
 - [19] Antropov V P, van Schilfgaarde M and Harmon B N 1995 *J. Magn. Magn. Mater.* **140–144** 1355
 - [20] Kübler J, Höck K H and Sticht J 1988 *J. Appl. Phys.* **63** 3482
 - [21] Lorenz R *et al* 1995 *Phys. Rev. Lett.* **77** 3688
 - [22] Nordström L and Singh D J 1999 *Phys. Rev. Lett.* **76** 4420
 - [23] Blöchl P E 1994 *Phys. Rev. B* **50** 17 953
 - [24] Kresse G and Joubert D 1999 *Phys. Rev. B* **59** 1758
 - [25] Hobbs D, Kresse G and Hafner J 2000 *Phys. Rev. B* **62** 11 556
 - [26] Perdew J P and Zunger A 1981 *Phys. Rev. B* **23** 5048
 - [27] Perdew J P *et al* 1992 *Phys. Rev. B* **46** 6671